Magnetic State of Pyrochlore $Cd_2Os_2O_7$ Emerging from Strong Competition of Ligand Distortions and Longer-Range Crystalline Anisotropy

Nikolay A. Bogdanov,[1] Rémi Maurice,[2] Ioannis Rousochatzakis,[1] Jeroen van den Brink,[1,3] and Liviu Hozoi[1]

[1]*Institute for Theoretical Solid State Physics, IFW Dresden, Helmholtzstrasse 20, 01069 Dresden, Germany*

[2]*Theoretical Chemistry Group, Zernike Institute for Advanced Materials, Rijksuniversiteit Groningen, Nijenborgh 4, 9747 AG Groningen, The Netherlands*

[3]*Department of Physics, Technical University Dresden, 01062 Dresden, Germany*

(Received 8 October 2012; published 19 March 2013)

By many-body quantum-chemical calculations, we investigate the role of two structural effects—local ligand distortions and the anisotropic Cd-ion coordination—on the magnetic state of $Cd_2Os_2O_7$, a spin $S = 3/2$ pyrochlore. We find that these effects strongly compete, rendering the magnetic interactions and ordering crucially dependent on these geometrical features. Without trigonal distortions, a large easy-plane magnetic anisotropy develops. Their presence, however, reverses the sign of the zero-field splitting and causes a large easy-axis anisotropy ($D \simeq -6.8$ meV), which in conjunction with the antiferromagnetic exchange interaction ($J \simeq 6.4$ meV) stabilizes an all-in–all-out magnetic order. The competition uncovered here is a generic feature of pyrochlore magnets.

DOI: 10.1103/PhysRevLett.110.127206 PACS numbers: 75.30.Gw, 75.10.Dg, 71.15.Rf, 75.30.Et

Introduction.—Oxide compounds of the 5*d* elements are at the heart of intensive experimental and theoretical investigations in condensed-matter physics and materials science. The few different structural varieties displaying Ir ions in octahedral coordination and tetravalent $5d^5$ valence states, in particular, have set the playground for new insights into the interplay between strong spin-orbit interactions and electron correlation effects [1–3]. Equally intriguing but less investigated are pentavalent Os $5d^3$ oxides such as the pyrochlore $Cd_2Os_2O_7$ [4,5] and the perovskite $NaOsO_3$ [6,7]. Just as for the iridates, major open questions with respect to the osmates are the mechanism of the metal to insulator transition (MIT) and the nature of the low-temperature antiferromagnetic (AF) configuration. While initially a Slater-type picture has been proposed for the MITs in both $Cd_2Os_2O_7$ [4] and $NaOsO_3$ [6,7], alternative scenarios such as a Lifshitz transition in the presence of sizeable electron-electron interactions have been suggested as well very recently [8,9].

So far, theoretical investigations of the electronic structure of the Os $5d^3$ oxides have been carried out only as mean-field ground-state (GS) calculations within the local-density approximation [10] or the LDA + *U* model [6,8]. Here, we report the results of many-body quantum-chemical calculations for $Cd_2Os_2O_7$. We describe the local Os d^3 multiplet structure, the precise mechanism of second-order spin-orbit coupling (SOC) and zero-field splitting (ZFS), and determine the parameters of the effective spin Hamiltonian, i.e., the single-ion anisotropy (SIA), nearest-neighbor (NN) Heisenberg exchange, as well as the Dzyaloshinskii-Moriya (DM) interactions. The results indicate that basic electronic-structure parameters such as the SIA crucially depend on geometrical details concerning both the O and adjacent Cd ions. In particular, the anisotropic Cd-ion coordination lifts the degeneracy of the Os t_{2g} levels even in the absence of O-ion trigonal distortions and yields large ZFSs and an easy-plane magnetic anisotropy. A configuration with trigonally distorted O octahedra is, however, energetically more favorable, changes the sign of the ZFS, and thus gives rise to easy-axis anisotropy at the Os sites, which, in conjunction with the AF NN exchange, stabilizes the so-called all-in–all-out spin order. The competition between the two structural effects is a generic feature in 227 pyrochlores and opens new perspectives on the basic magnetism in these materials.

Os d^3 electron configuration, single-ion physics.—To investigate in detail the Os *d*-level electronic structure, multiconfiguration self-consistent-field (MCSCF) and multireference configuration-interaction (MRCI) calculations [11] were first performed on embedded clusters made of one reference OsO_6 octahedron, six adjacent Cd sites, and six NN OsO_6 octahedra. The farther solid-state environment was modeled as an one-electron effective potential, which in a ionic picture reproduces the Madelung field in the cluster region. All calculations were performed with the MOLPRO quantum-chemical software [12]. We employed energy-consistent relativistic pseudopotentials for Os [13] and Cd [14] and Gaussian-type valence basis functions from the MOLPRO library (see the Supplemental Material [15]).

From simple considerations based on crystal-field (CF) theory, the orbital GS for a d^3 ion in octahedral coordination is a singlet. Thus, neglecting SOC, the lowest electron configuration should be ${}^4A_2(t_{2g}^3)$. This is indeed found in the quantum-chemical calculations if SOC is not included. The components of the spin-quartet A_2 GS can interact, however, via SOC with higher-lying T_2 terms and for noncubic axial systems split into two Kramers doublets

$m_S = \pm 1/2$ and $m_S = \pm 3/2$, respectively [16,17]. The T_2 states are themselves split in noncubic CFs. In the recent work of Matsuda *et al.* [5], for instance, the interaction of the $^4A_2$ and lowest $^4T_2$ states was analyzed. The *ab initio* quantum-chemical calculations yield, nevertheless, a rather large $^4A_2$-$^4T_2$ excitation energy, 5.4 eV by MCSCF calculations including in the active orbital space all $5d$ functions at the central Os site and the t_{2g} orbitals of the six Os NNs, which is not surprising in fact for extended $5d$ orbitals that feel very effectively the O $2p$ charge distribution. Additionally, the *ab initio* investigation actually shows that the excited ^2E and ^2T t_{2g}^3 doublets occur at much lower energies, from 1 to 2.5 eV (see Table I), and the ZFS of the $^4A_2$ levels is mainly related to the interaction with those states. To make the MRCI calculations feasible [18] and the analysis of the results limpid, we further replaced the six Os^{5+} d^3 NNs by closed-shell Ta^{5+} d^0 species. We checked, for example, that the $5d$ charge distribution and the t_{2g}-e_g splitting at the central Os site are not affected by this substitution. In the MRCI computations, we included on top of the MCSCF wave functions all single and double excitations from the Os $5d$ and O $2p$ orbitals at the central octahedron. The reference multiconfiguration active space is given by five $5d$ orbitals at the central Os site and three electrons, and the results are listed in Table I.

To extract the ZFS, we compute the spin-orbit interaction matrix for the lowest four quartet and three doublet spin states; see Table I. The MRCI + SOC data of Table I show that the ZFS of the $^4A_2$ GS is rather large, 13.5 meV. This gives a first estimate of the splitting parameter $|D| \approx 6.75$ meV, 1–2 orders of magnitude larger than for $3d$ ions in standard coordination [16,17]. However, for explicitly deriving the full SIA tensor $\bar{\bar{\mathbf{D}}}$, we further employ the effective Hamiltonian methodology described in Ref. [19]. Here, SOCs and the mixing of the $^4A_2$ components with higher-lying CF excited states are treated as small perturbations and the spin-orbit wave functions related to the high-spin t_{2g}^3 configuration are projected onto the space spanned by the $^4A_2$ $|S, M_S\rangle$ states. Using the orthonormalized projections $\tilde{\Psi}_k$ of the low-lying A_2 quartet wave functions and the corresponding eigenvalues E_k, we then construct the effective Hamiltonian $\hat{\mathcal{H}}_{\text{eff}} = \sum_k E_k |\tilde{\Psi}_k\rangle\langle\tilde{\Psi}_k|$ [19]. The orthonormalization is done using the formalism introduced by des Cloizeaux [20], i.e., $|\tilde{\Psi}_k\rangle = \mathbf{U}_{\text{ov}}^{-1/2} |\Psi_k\rangle$, where $\mathbf{U}_{\text{ov}}$ is the overlap matrix and $|\Psi_k\rangle$ are the projections of the wave functions onto the model space. A one-to-one correspondence can be now drawn between the matrix elements of $\hat{\mathcal{H}}_{\text{eff}}$ and the model Hamiltonian for the anisotropic single-site problem $\hat{\mathcal{H}}_{\text{mod}} = \mathbf{S} \cdot \bar{\bar{\mathbf{D}}} \cdot \mathbf{S}$ to extract the ZFS tensor (for details, see the Supplemental Material [15]). Diagonalizing the $\bar{\bar{\mathbf{D}}}$ tensor, we finally obtain on the basis of the *ab initio* quantum-chemical data an axial parameter $D = -6.77$ meV, a rhombic parameter $E = 0.0$, and an univocally defined easy axis of magnetization along the [111] direction, perpendicular to the plane of Cd NNs; see Fig. 1.

To gain deeper insight into the origin of the strong axial anisotropy, we performed additional calculations for an ideal pyrochlore structure with no trigonal distortions of the O octahedra. It turns out that the 227 pyrochlore lattice is fully defined by just three parameters: the space group, the cubic lattice constant a, and the coordinate x of the O at the $48f$ site, denoted as O(1) in Ref. [4]. For $x = x_0 = 5/16$, the oxygen cage around each Os site forms an undistorted, regular octahedron [21]. In $Cd_2Os_2O_7$, however, x is slightly larger than x_0 [4], which translates into a compressive trigonal distortion of the OsO_6 octahedra. Interestingly, for undistorted O octahedra (i.e., $x = x_0$), we still found $E = 0$ and the same orientation of the magnetic z axis. The axial parameter, however, changes its sign to $D = 2.50$ meV. A positive D indicates that the z axis is now a hard axis. The basic mechanism responsible for this change of sign is apparent when comparing the Os $5d^3$ multiplet structure for the actual lattice (Table I) with that for a idealized crystal with no trigonal distortions (Table II). In particular, the order of the split components of the $^2T_1$ states, i.e., one singly degenerate and one doubly

TABLE I. MRCI and MRCI + SOC relative energies (eV) for the Os^{5+} $5d^3$ multiplet structure in $Cd_2Os_2O_7$. Since cubic symmetry is lifted, the T states are split even without SOC. Each MRCI + SOC value stands for a spin-orbit doublet; for the ^4T states, only the lowest and highest components are shown.

$5d^3$ splittings	MRCI	MRCI + SOC ($\times 2$)
$^4A_2$ (t_{2g}^3)	0.00	0.00; 13.5×10^{-3}
^2E (t_{2g}^3)	1.51; 1.51	1.40; 1.53
$^2T_1$ (t_{2g}^3)	1.61; 1.62; 1.62	1.63; 1.66; 1.76
$^2T_2$ (t_{2g}^3)	2.46; 2.49; 2.49	2.63; 2.76; 2.87
$^4T_2$ ($t_{2g}^2 e_g^1$)	5.08; 5.20; 5.20	5.14; . . . ; 5.45
$^4T_1$ ($t_{2g}^2 e_g^1$)	5.89; 6.01; 6.01	6.02; . . . ; 6.33
$^4T_1$ ($t_{2g}^1 e_g^2$)	10.29; 10.63; 10.63	10.41; . . . ; 11.00

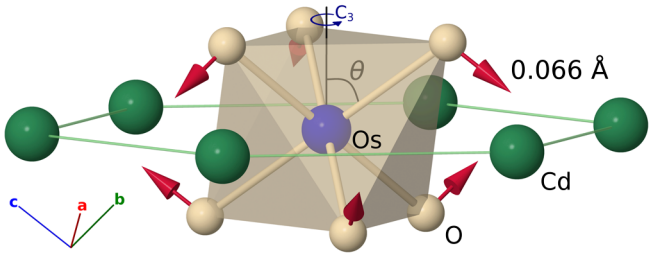

FIG. 1 (color online). Sketch of (i) the compressive trigonal distortion in $Cd_2Os_2O_7$ (red arrows) involving the O ligands (in beige) around each Os site (blue sphere) and (ii) the hexagonal Cd-ion (green spheres) coordination. The clusters used in the calculation of the ZFSs also include the six NN octahedra; see the text.

TABLE II. MRCI and MRCI + SOC relative energies (eV) for the Os^{5+} $5d^3$ multiplet structure in a hypothetical crystal with no trigonal distortions. Each MRCI + SOC value stands for a spin-orbit doublet; for the ^4T states, only the lowest and highest components are shown.

$5d^3$ splittings	MRCI	MRCI + SOC ($\times 2$)
$^4A_2$ (t_{2g}^3)	0.00	0.00; 5.00×10^{-3}
^2E (t_{2g}^3)	1.53; 1.53	1.43; 1.50
$^2T_1$ (t_{2g}^3)	1.61; 1.61; 1.63	1.64; 1.64; 1.75
$^2T_2$ (t_{2g}^3)	2.42; 2.45; 2.45	2.59; 2.75; 2.81
$^4T_2$ $(t_{2g}^2 e_g^1)$	5.34; 5.41; 5.41	5.36; . . . ; 5.65
$^4T_1$ $(t_{2g}^2 e_g^1)$	6.13; 6.20; 6.20	6.23; . . . ; 6.52
$^4T_1$ $(t_{2g}^1 e_g^2)$	10.85; 10.98; 10.98	10.93; . . . ; 11.38

degenerate term, changes in Table II as compared to Table I, which modifies the interaction of the A_2 terms with the excited states.

We find in the MRCI calculations a linear relation between D and the distortion angle $\Delta\theta$; see Fig. 2. The effect of a trigonal field alone on the energy levels and on the ZFS of d^3 ions has been previously investigated in the framework of a simplified CF model and perturbation theory [17,22]. A linear relation is also established in alum salts [22]. In contrast to the model assumed in Ref. [22], however, we find that the $D(\Delta\theta)$ line does not go through the origin. This is due to the noncubic field generated by the Cd NNs, which form a highly anisotropic planar structure around each Os site. Similar competing structural effects have been evidenced in Ni^{II}-Y^{III} molecular complexes [23]. We also plot in Fig. 2 the total-energy landscape as a function of the distortion angle $\Delta\theta$. It is seen that at the MRCI level the minimum of the parabola corresponds to a trigonal compressive distortion $\Delta\theta = 1.7°$ for a fixed Os-O bond length, close to the experimental value of 1.9° [4].

Superexchange interactions.—To investigate the NN magnetic couplings, we designed ten-octahedra embedded clusters. The analysis of the intersite interactions is here carried out for only two magnetically active Os d^3 ions (see Fig. 3), while for simplicity the eight Os^{5+} NNs were modeled as closed-shell Ta^{5+} d^0 ions. Multiconfiguration wave functions were first generated by state-averaged MCSCF optimizations for the lowest singlet, triplet, quintet, and septet states in the two-site problem. Those configuration state functions give rise in the spin-orbit calculations to sixteen spin-orbit states. For each spin multiplicity, the MCSCF active space is defined by the set of six Os t_{2g} orbitals accommodating a total number of six electrons. We then further accounted for single and double excitations from the Os t_{2g} and bridging-O $2p$ orbitals on top of the MCSCF reference wave functions. Such MRCI calculations yield magnetic coupling constants in very good agreement with experimental data in the $5d^5$ iridate Sr_2IrO_4 [24]. Similar strategies of explicitly dealing only with selected groups of localized ligand orbitals were adopted in earlier studies on $3d$ compounds [25].

From the calculations without SOCs, we see that the energy splittings between the different spin states follow the sequence J, $3J$, $6J$ and can be fitted to an AF isotropic exchange model $\hat{\mathcal{H}}_{\mathrm{AF}} = J\mathbf{S}_1 \cdot \mathbf{S}_2$, with a root-mean-square error of 0.3 meV. Adding a biquadratic term $K(\mathbf{S}_1 \cdot \mathbf{S}_2)^2$ improves the accuracy of the fit to 0.01 meV and yields a first MRCI estimate of $J = 6.42$ meV. Thus, J is of the same order of magnitude as the SIA while $K = 0.07$ meV.

Antisymmetric exchange.—Anisotropic, non-Heisenberg terms can be further obtained from spin-orbit calculations within the manifold defined by the lowest singlet, triplet, quintet, and septet spin states for two Os d^3 sites. As expected, including SOCs does not bring significant corrections to the effective superexchange: J is 6.43 meV by MRCI + SOC calculations. The spin-orbit interactions, however, lift the degeneracy of the initial spin multiplets

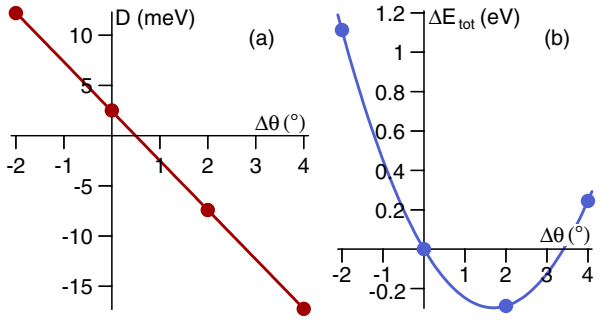

FIG. 2 (color online). (a) Single-ion anisotropy parameter D and (b) total energy of the cluster ΔE_{tot}, as functions of the trigonal distortion angle $\Delta\theta$; see the text. MRCI + SOC results for clusters such as that depicted in Fig. 1. No trigonal distortions are applied within the embedding, i.e., $x = x_0 = 5/16$ for the surrounding lattice.

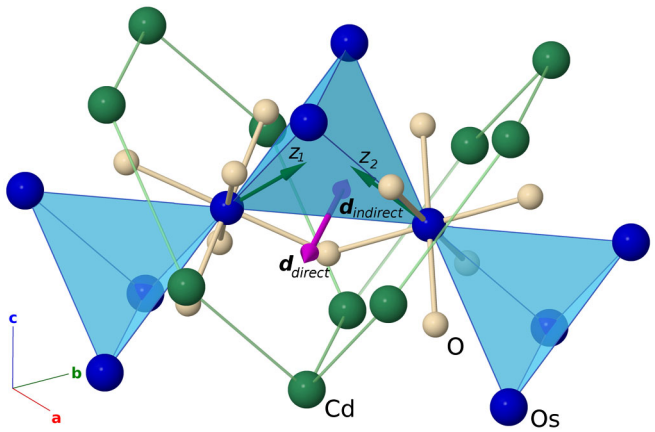

FIG. 3 (color online). Network of corner-shared Os_4 tetrahedra [shaded (blue) areas] in $Cd_2Os_2O_7$. O ligands and NN Cd ions around two adjacent Os sites are included. The two possible orientations of the DM vector [26] for two adjacent Os ions are also shown, along with their respective easy axes.

and bring in antisymmetric contributions. To describe the latter, we adopt a two-site model Hamiltonian $\hat{\mathcal{H}}'_{\mathrm{mod}}$ containing, in addition to the Heisenberg and biquadratic terms, a DM antisymmetric exchange contribution $\mathbf{d} \cdot \mathbf{S}_1 \times \mathbf{S}_2$, where $\mathbf{d}$ is a pseudovector with components d_x, d_y, and d_z. This model is then compared with the *ab initio* 16×16 effective matrix $\hat{\mathcal{H}}'_{\mathrm{eff}}$ derived from the MRCI + SOC calculations [15]. We found a perfect one-to-one correspondence between the two sets of matrix elements and could extract the numerical parameters $J = 6.43$, $K = 0.07$, and $\mathbf{d} = (1.17, -1.17, 0)$ meV. According to these results, the DM vector is oriented along the $\langle 110 \rangle$ directions (see Fig. 3 and Ref. [26]) and its norm is $|\mathbf{d}| = 1.65$ meV. The sense of the DM vector for a given Os-Os link, however, cannot be determined from our *ab intio* data.

Discussion.—Whereas the absolute value of the MRCI DM parameter is similar to estimates derived for certain values of the on-site Coulomb repulsion U by LDA + U calculations [8], the superexchange J and the SIA D turn out to be 2 (J) to 7 (D) times smaller in our quantum-chemical study. It is known that quantum-chemical calculations based on either configuration-interaction techniques or second-order perturbation theory are able to reproduce the experimentally derived J coupling constants with an accuracy better than $\pm 20\%$ in insulating $3d$-metal oxides; see, e.g., Refs. [25,27]. For more extended $5d$ electronic states in $5d$-metal oxides, the Hubbard U is neither small nor large compared to the bandwidth, as corroborated from the MITs [4,7] and from constrained local-density approximation calculations [6,8,28]. Electron itineracy may therefore pose additional technical problems and limit the applicability of a finite cluster approach. It has been shown, however, that accurate J's [24] and d-d excitation energies [29] can indeed be computed for $5d$ oxides such as the iridates. Those findings in Refs. [24,29] indicate that approaching the essential physics in the $5d$ oxides from a more localized perspective and within a finite-fragment framework certainly is a good starting point. Additional potentially problematic points concern the size of the clusters, as discussed, e.g., in Ref. [30]. The clusters we employ here are, however, large enough to ensure an accurate description of both the charge distribution of NN octahedra around the "active" d sites and the tails at those neighboring sites of Wannier-like orbitals in the active region. As concerns the SIA at d-metal sites in solids, extensive quantum-chemical investigations are missing. The present investigation therefore constitutes a step toward filling this gap.

The pure AF Heisenberg model on the pyrochlore lattice has an extensive number of classical GSs which prevent any Néel-type ordering down to zero temperature [31,32]. The easy-axis anisotropy lifts this macroscopic degeneracy and selects the so-called all-in–all-out (or its time reversed) state, whereby all four spins sharing a given tetrahedron point toward or away from its center. This GS is selected irrespective of the relative strength of the anisotropy and AF exchange energy [33]. Now, since the macroscopic GS degeneracy is already lifted by the SIA, including the smaller DM interactions is not expected to drastically modify the physics of the system. In fact, if the sign of the $\mathbf{d}$ vector is that of the direct type (as defined by Elhajal *et al.* [26]), the DM interaction also favors the all-in–all-out state and thus does not compete with the SIA. The competition arises for the opposite sign of the $\mathbf{d}$ vector, labeled as of indirect type in Ref. [26], where the DM couplings favor a continuous family of coplanar and non-coplanar GSs [26].

Conclusions.—While trigonal distortions of the ligand cage are believed to open the door to topologically insulating states in $j = 1/2$ 227 iridate pyrochlores [2,28,34], we show here that the lattice degrees of freedom can fundamentally modify the nature of the magnetic interactions and ground states in $5d$ 227 compounds with larger magnetic moments. For this, we employ *ab initio* multireference configuration-interaction methods, the results of which are further mapped onto model Hamiltonians including both isotropic and anisotropic terms. To extract the DM couplings, we have expanded the formalism proposed earlier for $S = 1/2$ cuprates [35]. For the experimentally determined crystal structure of $Cd_2Os_2O_7$ [4], we find an AF superexchange coupling $J = 6.43$ meV and easy-axis anisotropy of the same magnitude $D = -6.77$ meV, while the DM parameter is 3–4 times smaller. The dominant magnetic interactions J and D give rise to the all-in–all-out AF order [26,33]. Most remarkably, the hexagonal Cd-ion coordination induces electrostatic fields that compete with the compressive trigonal distortion of the O octahedra that is present in the system. If the latter is removed, the SIA turns positive; i.e., D reverses sign and the system develops easy-plane magnetic anisotropy. This obviously implies qualitatively different magnetic properties [36]. Our findings thus indicate that there is in 227 pyrochlores a transition from unfrustrated to highly frustrated magnetism controlled by the amount of trigonal distortion. The latter can in principle be varied by changing either the A-site or B-site ions in the $A_2B_2O_7$ compounds, replacing for instance Cd (Os) by Hg (Re) [21], and is in addition tunable by applying pressure. For a correct understanding of such magnetic interactions, ordering tendencies, and transitions, the subtle interplay between oxygen- and A-ion anisotropic electrostatic effects is essential.

R. M. and L. H. thank Ria Broer for inspiring and insightful discussions and constant ongoing collaboration. We also thank V. M. Katukuri, R. Ganesh, H. Stoll, and P. Fulde for fruitful discussions. N. A. B. and L. H. acknowledge financial support from the Erasmus Mundus Programme of the European Union and the German Research Foundation (Deutsche Forschungsgemeinschaft, DFG), respectively.

[1] B. J. Kim, H. Ohsumi, T. Komesu, S. Sakai, T. Morita, H. Takagi, and T. Arima, Science **323**, 1329 (2009).

[2] D. Pesin and L. Balents, Nat. Phys. **6**, 376 (2010).

[3] J. Chaloupka, G. Jackeli, and G. Khaliullin, Phys. Rev. Lett. **105**, 027204 (2010).

[4] D. Mandrus, J. R. Thompson, R. Gaal, L. Forro, J. C. Bryan, B. C. Chakoumakos, L. M. Woods, B. C. Sales, R. S. Fishman, and V. Keppens, Phys. Rev. B **63**, 195104 (2001).

[5] Y. H. Matsuda, J. L. Her, S. Michimura, T. Inami, M. Suzuki, N. Kawamura, M. Mizumaki, K. Kindo, J. Yamauara, and Z. Hiroi, Phys. Rev. B **84**, 174431 (2011).

[6] Y. G. Shi, Y. F. Guo, S. Yu, M. Arai, A. A. Belik, A. Sato, K. Yamaura, E. Takayama-Muromachi, H. F. Tian, H. X. Yang, J. Q. Li, T. Varga, J. F. Mitchell, and S. Okamoto, Phys. Rev. B **80**, 161104 (2009).

[7] S. Calder, V. O. Garlea, D. F. McMorrow, M. D. Lumsden, M. B. Stone, J. C. Lang, J.-W. Kim, J. A. Schlueter, Y. G. Shi, K. Yamaura, Y. S. Sun, Y. Tsujimoto, and A. D. Christianson, Phys. Rev. Lett. **108**, 257209 (2012).

[8] H. Shinaoka, T. Miyake, and S. Ishibashi, Phys. Rev. Lett. **108**, 247204 (2012).

[9] J. Yamaura, K. Ohgushi, H. Ohsumi, T. Hasegawa, I. Yamauchi, K. Sugimoto, S. Takeshita, A. Tokuda, M. Takata, M. Udagawa, M. Takigawa, H. Harima, T. Arima, and Z. Hiroi, Phys. Rev. Lett. **108**, 247205 (2012).

[10] D. J. Singh, P. Blaha, K. Schwarz, and J. O. Sofo, Phys. Rev. B **65**, 155109 (2002).

[11] T. Helgaker, P. Jørgensen, and J. Olsen, *Molecular Electronic-Structure Theory* (Wiley, Chichester, 2000); P. Fulde, *Correlated Electrons in Quantum Matter* (World Scientific, Singapore, 2012).

[12] H.-J. Werner, P. J. Knowles, G. Knizia, F. R. Manby, and M. Schütz, computer code MOLPRO, 2010, http://www.molpro.net.

[13] D. Figgen, K. A. Peterson, M. Dolg, and H. Stoll, J. Chem. Phys. **130**, 164108 (2009).

[14] F. Schautz, H.-J. Flad, and M. Dolg, Theor. Chem. Acc. **99**, 231 (1998).

[15] See Supplemental Material at http://link.aps.org/supplemental/10.1103/PhysRevLett.110.127206 for the basis set details and for the effective and expanded model Hamiltonians.

[16] R. Boča, Coord. Chem. Rev. **248**, 757 (2004).

[17] R. M. Macfarlane, J. Chem. Phys. **47**, 2066 (1967); **39**, 3118 (1963).

[18] The size of the MRCI expansion is reduced in that way by a few orders of magnitude.

[19] R. Maurice, R. Bastardis, C. de Graaf, N. Suaud, T. Mallah, and N. Guihéry, J. Chem. Theory Comput. **5**, 2977 (2009).

[20] J. des Cloizeaux, Nucl. Phys. **20**, 321 (1960).

[21] M. A. Subramanian, G. Aravamudan, and G. V. S. Rao, Prog. Solid State Chem. **15**, 55 (1983).

[22] Y.-F. Li, X.-Y. Kuang, M.-L. Gao, Y.-R. Zhao, and H.-Q. Wang, Chin. Phys. B **18**, 2967 (2009).

[23] R. Maurice, L. Vendier, and J.-P. Costes, Inorg. Chem. **50**, 11 075 (2011).

[24] V. M. Katukuri, H. Stoll, J. van den Brink, and L. Hozoi, Phys. Rev. B **85**, 220402 (2012).

[25] K. Fink, R. Fink, and V. Staemmler, Inorg. Chem. **33**, 6219 (1994); C. J. Calzado, S. Evangelisti, and D. Maynau, J. Phys. Chem. A **107**, 7581 (2003); R. Broer, L. Hozoi, and W. C. Nieuwpoort, Mol. Phys. **101**, 233 (2003).

[26] M. Elhajal, B. Canals, R. Sunyer, and C. Lacroix, Phys. Rev. B **71**, 094420 (2005).

[27] D. Muñoz, I. de P. R. Moreira, and F. Illas, Phys. Rev. B **65**, 224521 (2002); C. de Graaf, R. Broer, and W. C. Nieuwpoort, Chem. Phys. Lett. **271**, 372 (1997); L. Hozoi, C. Presura, C. de Graaf, and R. Broer, Phys. Rev. B **67**, 035117 (2003).

[28] X. Wan, A. M. Turner, A. Vishwanath, and S. Y. Savrasov, Phys. Rev. B **83**, 205101 (2011).

[29] X. Liu, V. M. Katukuri, L. Hozoi, W.-G. Yin, M. P. M. Dean, M. H. Upton, J. Kim, D. Casa, A. Said, T. Gog, T. F. Qi, G. Cao, A. M. Tsvelik, J. van den Brink, and J. P. Hill, Phys. Rev. Lett. **109**, 157401 (2012); H. Gretarsson, J. P. Clancy, X. Liu, J. P. Hill, E. Bozin, Y. Singh, S. Manni, P. Gegenwart, J. Kim, A. H. Said, D. Casa, T. Gog, M. H. Upton, H.-S. Kim, J. Yu, V. M. Katukuri, L. Hozoi, J. van den Brink, and Y.-J. Kim, Phys. Rev. Lett. **110**, 076402 (2013); L. Hozoi, H. Gretarsson, J. P. Clancy, B.-G. Jeon, B. Lee, K. H. Kim, V. Yushankhai, P. Fulde, Y.-J. Kim, and J. van den Brink, arXiv:1212.4009.

[30] L. Hozoi, L. Siurakshina, P. Fulde, and J. van den Brink, Sci. Rep. **1**, 65 (2011).

[31] J. N. Reimers, Phys. Rev. B **45**, 7287 (1992); J. N. Reimers, A. J. Berlinsky, and A.-C. Shi, Phys. Rev. B **43**, 865 (1991).

[32] R. Moessner and J. T. Chalker, Phys. Rev. Lett. **80**, 2929 (1998); Phys. Rev. B **58**, 12 049 (1998).

[33] R. Moessner, Phys. Rev. B **57**, R5587 (1998).

[34] B.-J. Yang and Y. B. Kim, Phys. Rev. B **82**, 085111 (2010).

[35] R. Maurice, A. M. Pradipto, N. Guihéry, R. Broer, and C. de Graaf, J. Chem. Theory Comput. **6**, 3092 (2010); A. M. Pradipto, R. Maurice, N. Guihéry, C. de Graaf, and R. Broer, Phys. Rev. B **85**, 014409 (2012); R. Maurice, A.-M. Pradipto, C. de Graaf, and R. Broer, Phys. Rev. B **86**, 024411 (2012).

[36] S. T. Bramwell, M. J. P. Gingras, and J. N. Reimers, J. Appl. Phys. **75**, 5523 (1994); J. D. M. Champion and P. C. W. Holdsworth, J. Phys. Condens. Matter **16**, S665 (2004).